Realization of Task Intelligence Based on the Intelligence Operating Architecture for Assistive Robots

Bum-Soo Yoo, Yong-Ho Yoo, Woo-Ri Ko, Seung-Jae Lee, Seung-Hwan Baek, Se-Hyoung Cho, and Jong-Hwan Kim
School of Electrical Engineering, KAIST
291 Daehak-ro, Yuseong-gu, Daejeon 305-701, Republic of Korea

Abstract— *Various types of robots have been built and used in our daily life for various purposes. One of them is an assistive robot that can autonomously perform a proper task in a given situation. The robot is required to integrate constituent algorithms into one controlled architecture for the autonomous operation. In this paper, we categorize the constituent algorithms that are developed for functional purposes of assistive robots and integrate them into the intelligence operating architecture to realize task intelligence for the robots. The effectiveness and applicability of the integrated architecture is demonstrated through the experiments with the humanoid robot, Mybot-KSR, developed in the Robot Intelligence Technology Lab., at KAIST.*

Keywords: Adaptive resonance theory (ART), humanoid robot, intelligence operating architecture (iOA), knowledge architecture, mechanism of thought, task intelligence.

1. Introduction

Robots have been used in our daily life for various purposes, such as entertainment, human-aid, personal assistance, etc. Even though it has not been long since robots' introduction in our daily life, robots are already considered capable of making human life more productive and delightful. Among them, personal assistive robots are designed to support humans in their homes and offices. To stay close with humans, they should look friendly to humans and also think and behave as the humans do. Thinking mechanism of the personal assistive robots needs to be engineered similar to human reasoning process since the human intelligence is yet known to be the most efficient for reasoning to generate a sequence of procedures.

The crux of building personal assistive robots is to integrate several constituent algorithms into one controlled architecture, which makes robots autonomously generate a proper behavior in a given situation. Considerable research has been performed in this area. An ontology-based unified robot knowledge framework for integration of low-level data with high-level knowledge was introduced [1]. A robot system producing behaviors from human activities was suggested [2]. It learned human activities and their interactions with objects in the form of associated affordances. Also, an autonomous robot system to learn manipulation action plans was introduced [3]. It used videos from the World Wide Web with convolutional neural network (CNN) and probabilistic manipulation action grammar based parsing module. However, none of these studies presented an integration of memorizing feature as in human brain with other features under high-level architecture controlled with intelligence in more human-like manner.

In this paper, we realize an integrated task intelligence using the intelligence operating architecture (iOA) for the humanoid robot, Mybot-KSR [4]. The iOA is based on the key functions of human brain to develop robot intelligence by governing the five constituent parts: perception, internal state, memory, reasoning, and execution. The robot uses the perception part to perceive environment. The perception module recognizes task-related objects by the CNN [5]. The memory part retrieves the most adequate task from the recognized objects using the adaptive resonance theory (ART), which is followed by retrieving a sequence of procedures for the task [6]-[8]. The robot constructs the ART structure by learning and memorizing the inter-connectivity between situations and tasks, including the sequence of procedures. The reasoning part generates behaviors for performing a task. Each procedure of the task in the memory part can retrieve a proper behavior with objects, which is sub-divided into executable forms, called primitive behaviors. The behavior selection module generates a sequence of primitive behaviors using the degree of consideration-based mechanism of thought (DoC-MoT) [9]. The behavior generation module produces trajectories for performing primitive behaviors with the rapidly-exploring random tree star (RRT*) [10]. Not only the trajectories from the RRT*, the trajectories learned from human behaviors are also used if trajectories are hard to be expressed with points and angles [11]. Besides, the attention module makes the perception more efficiently by controlling the gaze of the robot with a state machine [12]. Finally, the execution part controls motors to generate behaviors of the robot. Results of behaviors are perceived again to update robots behaviors continuously. Note that since the internal state part is not highly related with tasks, it is not used in this paper.

This paper is organized as follows. Section II presents realization of the iOA with constituent algorithms. Section III describes the experimental results with the Mybot-KSR.

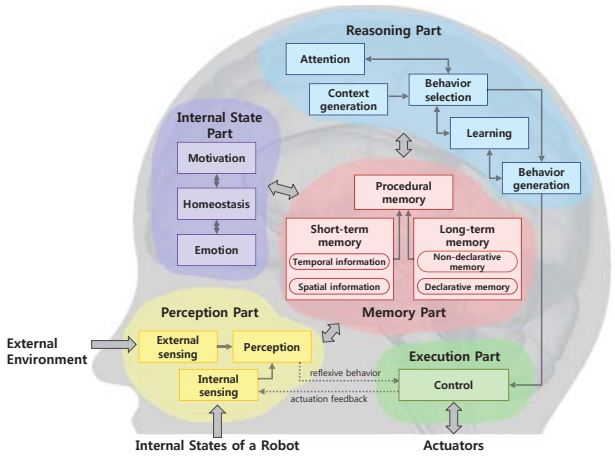

Fig. 1: The intelligence operating architecture.

Finally, the conclusion remarks follow in Section IV.

2. Intelligence Operating Architecture

Fig. 1 shows the intelligence operating architecture to integrate the constituent algorithms for realizing task intelligence of robots. It consists of five parts with fifteen modules. The perception part perceives environment and recognizes task-related objects. The memory part retrieves the most adequate task from the recognized objects. It also retrieves a sequence of procedures for performing tasks. The reasoning part subdivides a sequence of procedures into executable forms. Finally, the execution part controls motors to perform the proper task.

2.1 Perception Part

The robot can perceive external environment with the RGB-D camera through the external sensing module. The perceived visual inputs are delivered to the perception module. Task-related objects are recognized and their information is delivered to the memory part and reasoning part to perform tasks. Note that since the internal state part is not highly related to tasks, it is excluded along with the internal sensing module from the perception part.

In the perception module, a plane in the visual input is found by the random sample consensus (RANSAC) algorithm [13]. Since objects are usually placed on a plane the pixel points in and under the plane are filtered, while the rest points are regarded as objects. Along with it, the CNN for object recognition is actualized by the Convolutional Architecture for Fast Feature Embedding (CAFFE) library. The CNN is a series of layers consisting of neurons. Each neuron in hidden layers is assigned to a part of input neurons, called receptive field, and the CNN recognizes objects based on the receptive field only. As the information is fed forward, the outputs of neurons at each layer are gradually pooled. Also, the receptive field becomes larger, and the recognition becomes more accurate. Unlike the conventional recognition algorithm that tried to design good feature descriptors to extract important information, the CNN has a strong point in learning feature extraction by itself using perceived visual inputs only [5].

2.2 Memory Part

Robots are expected to autonomously infer the most adequate task from its memory for a perceived situation. Also, they need to retrieve a proper sequence of procedures from the memory to perform the task, which is called procedural memory. The procedural memory has been developed based on the ART [7]. The ART structure can memorize interconnectivity between situations and tasks, including the sequence of procedures.

The structure of the adaptive resonance system is shown in Fig. 2. It consists of an input field (F_1), procedure field (F_2), and task field (F_3). The F_1 field receives perceived input from the perception part. In this paper, it encodes the perceived input into five channels: a moving object (F_1^1), an aimed object (F_1^2), a relative position between the moving object and the aimed object (F_1^3), an inclination of the moving object (F_1^4), and an action performed by the moving object (F_1^5). The moving objects are {*bread, toy, bottle, watering pot*}, the aimed objects are {*toaster, dish, box, bowl, flowerpot*}, and the behaviors are {*grasp, move, tilt, put down, push down, pour*}.

The k-th channel is represented as the input vector $\mathbf{Z}^k = [z_1^k \; z_2^k \; \dots \; z_{n_k}^k]^T$, where n_k is the number of nodes in the k-th channel and $z_i^k \in [0,1]$, i=1, 2, . . . , n_k, indicates a value of the i-th node. Each node in F_1^1, F_1^2, and F_1^5 represents whether objects and action are perceived or not, respectively. Each node in F_1^3 represents the relative position between the moving object and the aimed object along the horizontal, vertical axes, normalized by 10.0 m. A relative depth position is also included. Each node in F_1^4 represents the inclination of the moving object along the roll, pitch, and yaw axes, normalized by π. The input vector $\mathbf{Z}^k$ is converted to an activity vector $\mathbf{X}^k$ by concatenation of the input vector $\mathbf{Z}^k$ and its complements $\bar{\mathbf{Z}}^k$. The F_2 field has one channel, which is represented as $\mathbf{Y} = [y_1 \; y_2 \; \dots \; y_m]^T$, where m is the number of nodes in F_2 field and $y_j \in [0,1]$, j=1, 2, . . . , m, indicates whether the j-th procedure occurs or not. The j-th node in F_2 field is evaluated with respect to each channel as follows:

$$T_j = \sum_{k=1}^{5} \gamma^k \frac{(\mathbf{X}^k \wedge \mathbf{W}_j^k)}{\alpha^k + |\mathbf{W}_j^k|} \tag{1}$$

where $\alpha^k \geq 0$ is a user-defined bias parameter, $\gamma^k \in [0,1]$ is a user-defined contribution parameter for k-th channel, and $\mathbf{W}_j^k = [w_{j_1}^k \; w_{j_2}^k \; \dots \; w_{j_{2n_k}}^k]^T$ is a weight vector between the channel k of the F_1 field and the channel of the F_2 field. The $P \wedge Q$ for $P = [p_1 \; p_2 \; \dots \; p_u]^T$ and $Q = [q_1 \; q_2 \; \dots \; q_u]^T$ is defined as $\sqrt{\sum_{i=1}^{u} (\min(p_u, q_u))^2}$. The node of the largest

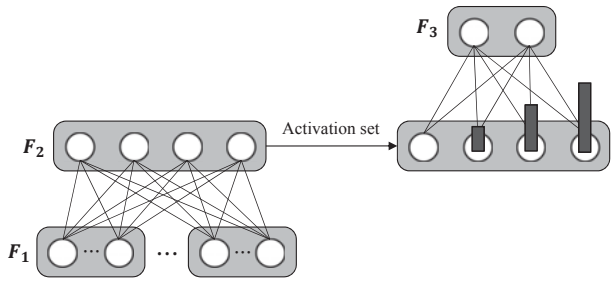

Fig. 2: The adaptive resonance system consists of three fields: the input field F_1, procedure field F_2, and task field F_3.

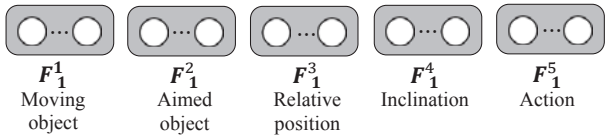

Fig. 3: A set of input vector in each channel.

T_j value is selected, and the resonance is evaluated as follows:

$$M^k = \frac{(\mathbf{X}^k \wedge \mathbf{W}^k_{j_{max}})}{\left|\mathbf{X}^k\right|} \tag{2}$$

where j_{max} is the selected node of the largest T_j value.

When the M^k is greater than the user defined vigilance parameter ρ^k for all k, the resonance occurs and $\mathbf{W}^k_{j_{max}}$ is updated as follows:

$$\mathbf{W}^{k(t+1)}_{j_{max}} = (1-\beta^k)\mathbf{W}^{k(t)}_{j_{max}} + \beta^k \min(\mathbf{x}^k, \mathbf{W}^{k(t)}_{j_{max}}) \tag{3}$$

where $\beta^k \in [0,1]$ is the user-defined learning rate of the k-th channel. If the resonance does not occur for all k, a new node is committed in the F_2 field.

In the learning process, the committed nodes in the F_2 field produce an activation set in the same F_2 field. The activation set is input to produce nodes in the F_3 field, as the F_1 field produces nodes in the F_2 field. The robot memorizes procedures of tasks by the nodes and weights, and uses them to recognize which task is adequate in a given situation.

2.3 Reasoning Part

2.3.1 Behavior Selection Module

After retrieving a sequence of procedures from the memory part, the behavior selection module provides a series of primitive behaviors to complete each procedure and select one of them considering situational information along with the degree of consideration for the information. For example, to accomplish the "grasping a bottle" procedure, the robot should "look around" to find out where the target object is positioned. Then, if a target object is positioned out of reachable range of hands of the robot, firstly the robot should "approach" the target object to grasp. Four situational

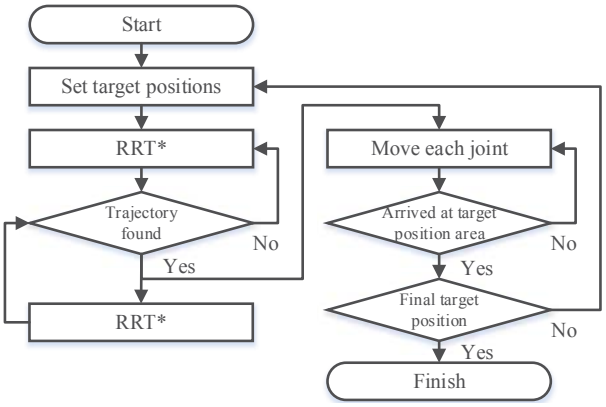

Fig. 4: The flowchart of an arm trajectory generation.

information and seven primitive behaviors can be defined respectively as shown in Table 1 and Table 2.

Table 1: Example of situational information.

	Situational information	Unit	Range
1	The distance between the robot's upper body and the target object (s_1)	m	[0,5]
2	The distance between the robot's hand and the target object (s_2)	m	[0,5]
3	The distance between the current and target positions of the grasping object (s_3)	m	[0,5]
4	The difference between the current and target orientation of the grasping object (s_4)	°	[0, 360]

Table 2: Example of primitive behaviors.

	Contents
Primitive behaviors	Look around (b_1), approach (b_2), bend body (b_3), grasp (b_4), move (b_5), tilt (b_6), pour (b_7)

The most appropriate sequence of primitive behaviors in a given situation is selected by the DoC-MoT [9]. The DoC is assigned to the power set of situational information with the λ-fuzzy measure [15]. Having the DoC applied, each primitive behavior, b_i, $i = 1, 2, \ldots, n$, is evaluated by the Choquet fuzzy integral as follows:

$$E(b_i) = \sum_{j=1}^{m} \{l_{ij} \cdot h^t_{ij} - l_{i(j-1)} \cdot h^t_{i(j-1)}\} g(S_j) \tag{4}$$

where $h_{ij} \in [0,1]$ is the user-defined partial evaluation value of b_i over j-th situational information s_j, m is the number of situational information, $L = (l_{ij})_{m \times n}$ is the knowledge link strength matrix in the learning module, and $g(S_j)$ is the DoC applied to S_j with assumptions that $h_{ij} \leq h_{i(j+1)}$ and $S_j = \{s_j, s_{j+1}, \ldots, s_n\}$. After evaluating all primitive behaviors, the primitive behavior of the largest evaluation value is selected and is transferred to the behavior generation module.

2.3.2 Learning Module

The robot requires a proper link strength matrix in (4) to perform correct primitive behaviors in a given situation. Since the robot does not know a suitability of its behaviors, it needs to use a user-recommended behavior to evaluate the suitability between behaviors and situations. All l_{ij} are initially assigned as 1.0 and is updated by the user-recommended behavior, b_r, as follows:

$$l_{rj}^{t+1} = l_{rj}^{t} + \eta h_{rj}^{t} \tag{5}$$

where $\eta \in [0, 1]$ is the learning rate. The trained knowledge link strength matrix is normalized to satisfy $\sum_{i,j} l_{ij} = 1$ and used in (4).

2.3.3 Behavior Generation Module

The robot needs to generate a trajectory of its arms to manipulate objects such as tilting, grasping, and pouring. The RRT* can be used to generate a trajectory [16]. The RRT* is one of sampling-based algorithms that can generate optimal collision-free trajectories [10]. Fig. 4 shows the flowchart of the arm trajectory generating algorithm. From the behavior selection module, a primitive behavior that requires movement of an arm is transferred. Then, the behavior generation module chooses a closer arm to the target position, and the RRT* algorithm searches for an optimal trajectory from the hand of the chosen arm to the target position. The robot starts to move its arm when the initial trajectory is produced, and it stops movement when the hand arrives at the target position. During the movement, the robot continuously calculates the current position of the hand to monitor whether it has arrived at the target position or not. At the same time, the RRT* algorithm updates continuously to generate the optimal trajectory. Note that, if a sequence of target positions is produced, the robot generates trajectory to each target position sequentially.

After arriving the final target position, the robot needs to perform the behaviors of not only grasping objects, but also performing tasks on the grasped objects. Unlike the trajectories generated by the RRT*, generating trajectories for the grasping object is sometimes as inconvenient to be expressed by a series of coordinates and angles as generating trajectories for shaking. The robot can learn behaviors for the task from human's demonstration. The Gaussian mixture model (GMM) extracts dynamic characteristics of the multiple trajectories from the human's demonstration, and the motion trajectory morphing (MTM) algorithm generates a modified behavior trajectory for current environment by maintaining the dynamic characteristics [11].

2.3.4 Attention Module

The robot should acquire information of its surrounding environment to successfully perform tasks. Paying attention to proper targets at the right time can be a good solution to acquire the information. Since the gaze represents where the robot is paying attention to, the attention module controls the gaze of the robot. The attention module allows the robot to acquire situational information to perform tasks with its limited field of view and to indicate that the robot is concentrating on current tasks [12], [17].

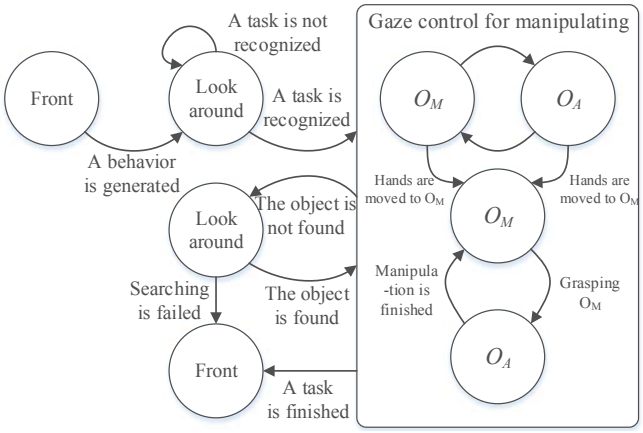

Fig. 5: A state machine in the attention module.

Most of people, who pursue the same goal, usually require similar information for the given task. It produces a large similarity in human gaze. Therefore, a state machine is used to designate targets for gazing in a sequence of procedures. Fig. 5 shows the state machine for the gaze control used in the experiments, where O_M and O_A represent the moving object and aimed object, respectively. At first, the robot gazes at the front. The behavior generation module in the reasoning part selects the "look around" behavior, and the robot starts looking around to perceive environment. From the perceived environment, the robot retrieves a sequence of procedures to perform a given task. Then, the robot performs its gaze control according to the state machine, until it finishes the task or the behavior generation module selects the "look around" behavior. The "look around" behavior is selected, when the objects disappear. The robot resumes the gaze control after detecting the objects, and it stops the gaze control when it fails to detect objects for a certain time period.

3. Experiments

3.1 Mybot-KSR

The Mybot-KSR is the humanoid robot developed in the Robot Intelligence Technology (RIT) Lab., at KAIST. Fig. 6 shows the Mybot-KSR and its configuration. The height of the robot is 142.0 cm and the weight is 58.0 kg. Degrees of freedom (DoFs) of each part is listed in Table 3. The robot is equipped with one RGB-D camera and four microphones on its head. The arms are built using integrated joint modules: a position sensor, a torque sensor, a motor and a harmonic

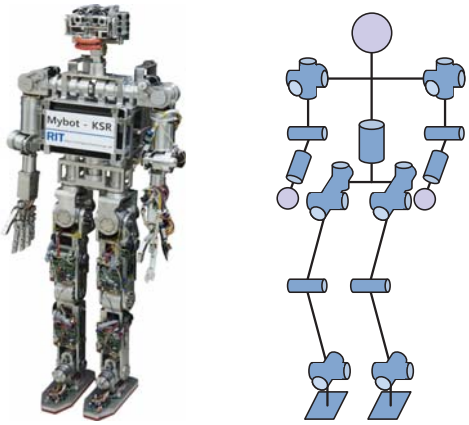

(a) (b)

Fig. 6: (a) The Mybot-KSR used in the experiment. (b) Configuration of the Mybot-KSR.

Table 3: Degrees of freedom of the Mybot-KSR.

Part	Arms	Hands	Head	Legs	Waist	Total
DoF	5×2	5×2	17	6×2	1	50

drive gear. The feet are mounted with a force-torque sensor to measure foot pressure.

Two PCs are used to control the robot. One with the i7-2670QM 2.2GHz CPU operates the iOA to decide behaviors from perceptive input, and the other with the Intel Atom N570 CPU controls posture by the 17 digital signal processors (DSPs), the TMS320C2846. The controller area network (CAN) are used to transfer control signals to the DSPs at every 10 ms, and each DSP controls motors at every 0.5 ms.

3.2 Experimental Results

The experiment was carried out in the lab environment. The robot had the yellow and red bottles, a mustard, and a bowl on the table in front of it. The robot inferred which task would be best fit in the given situation, mainly by identifying objects. Fig. 8 shows the snapshots of the experiments. On the first row are the images of the appearance of the robot with the table, and the second and third rows respectively show the RGB and depth images taken by the robot. In the RGB images, the detected objects, tracked object, and gaze direction are respectively marked with boxes, ellipses, and a circle. In the depth images, the plane is filtered out by the RANSAC, and a pair of images in each column were taken at the same time step. Note that in the RGB images, the bowl is supposed to be caught in the ellipse, but not due to its white color.

When the robot experienced difficulty in finding objects in its field of view it autonomously selected one of the primitive behaviors, "look around", to find objects. After looking around, robot had a set of objects in its field of view: the yellow and red bottles, mustard, and a bowl, as shown in Fig. 8(a). From the recognized objects, it retrieved a specific memory by the ART on pouring the liquid inside the red bottle into the bowl from the procedural memory. Fig. 7 describes the retrieved sequence of procedures and the selected primitive behaviors to accomplish each procedure. The robot utilized the four situational information in Table 1 to evaluate each primitive behavior in Table 2. Reaching out its hand toward the target object to realize it was far to grasp, the robot selected the "approach" primitive behavior. Fig. 8(b) shows the robot approaching the target object using the modifiable walking pattern generator [18]. The robot stopped approaching when it reached the area in which the target object is close enough to grasp.

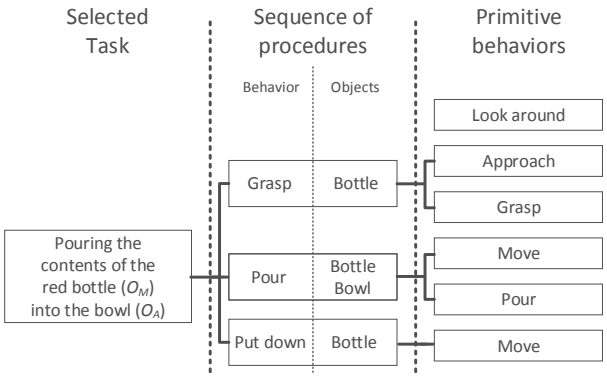

Fig. 7: The retrieved procedural memory with the sequence of procedures and the provided primitive behaviors.

To grasp the object, the robot chose the arm closer to the object and shifted the arm to the object using the RRT*, as shown in Fig. 8(c). For this movement, the robot used the "grasp" primitive behavior. With the help of the RRT*, the robot produced collision-free trajectories to avoid the table and other objects such as the yellow bottle. After grasping, the robot generated the "move" primitive behavior to take its arm above the bowl, followed by the "pour" primitive behavior, as shown in Figs. 8(d) and (e). Since the trajectories for the "pour" primitive behavior are inconvenient to be expressed by a series of coordinates and angles, they had previously been memorized through learning from human demonstration. The memorized behavior was modified suitable to the environment by the MTM algorithm. Finally, the robot replaced the red bottle to its original place and completed the task, as shown in Fig. 8(f). During the experiments, the robot produced appropriate gaze directions by the state machine.

4. Conclusion

In this paper, we developed and presented the iOA embedded robot system to carry out a given task with task intelligence. The iOA integrated constituent parts for key functions of human brain. This integrated iOA enabled to

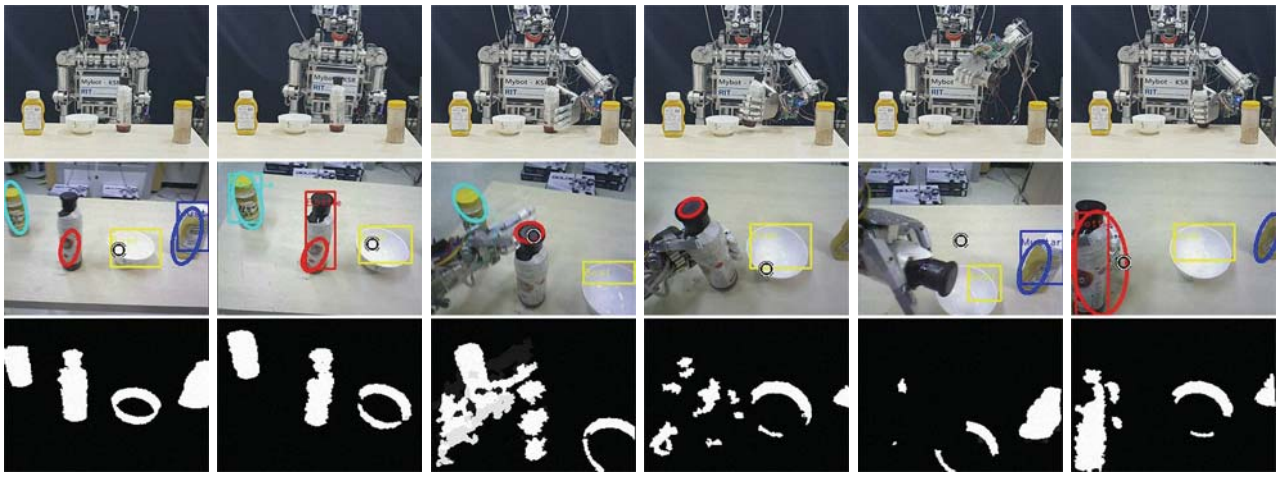

(a) (b) (c) (d) (e) (f)

Fig. 8: Snapshots of the experiments. (a) The Mybot-KSR looked around and found the objects. (b) The robot walked to the target object. (c) The robot moved the arm to the object. (d) The robot moved the grasped red bottle to the bowl. (e) The robot poured the contents of the red bottle into the bowl. (f) The robot finished its task by taking the red bottle back to its original place.

memorize detected objects and related human behaviors to pertain current situation with the corresponding sequence of procedures, and to retrieve a relevant set of primitive behaviors. The experimental results showed that the robot embedded with the integrated iOA autonomously retrieve a sequence of procedures for a task in a given situation and successfully completed it through the reasoning process.

Acknowledgement

This work was supported by the Technology Innovation Program, 10045252, supported by the Ministry of Trade, Industry, and Energy (MOTIE, Korea).

References

[1] G. H. Lim *et al.,* "Ontology-based unified robot knowledge for service robots in indoor environments," *IEEE Trans. Syst. Man Cybern. A., Syst. Humans,* vol. 41, no. 3, pp. 492-509, May 2011.

[2] H. S. Koppula, *et al.,* "Learning human activities and object affordances from rgb-d videos" *Int. J. Robot. Research*, vol. 32, no. 8, pp. 951-970, Jul. 2013.

[3] Y. Yang *et al.,* "Robot learning manipulation action plans by "watching"unconstrained videos from the world wide web," submitted for publication.

[4] J.-H. Kim, *et al.,* "Intelligence technology for robots that think," *IEEE Comput. Intell. Mag.,* vol. 8, no. 5, pp. 70-84, Aug. 2013.

[5] Y. LeCun *et al.*, "Gradient-based learning applied to document recognition," *Proc. IEEE,* vol. 86, no. 11, pp. 2278-2324, Nov. 1998.

[6] W. Wang, *et al.,* "Neural modeling of episodic memory: Encoding, retrieval, and forgetting," *IEEE Trans. Neural Netw. Learn. Syst.*, vol. 23, no. 10, pp. 1574-1586, Aug. 2012.

[7] Y.-H. Yoo and J.-H. Kim, "Procedural memory learning from demonstration for task performance" in *Proc. Int. Conf. Systems, Man, and Cybernetics,* Hong Kong, China, 2015, to be published.

[8] G.-M Park *et al.,* "REM-ART: Reward-based electromagnetic adaptive resonance theory" in *Proc. Int. Conf. Artificial Intelligence,* Las Vegas, NV, USA, 2015, to be published.

[9] J.-H. Kim *et al.*, "The degree of consideration-based mechanism of thought and its application to artificial creatures for behavior selection," *IEEE Comput. Intell. Mag.,* vol. 7, no. 1, pp. 49-63, Jan. 2012.

[10] S. Karaman and E. Frazzoli, "Sampling-based algorithms for optimal motion planning," *Int. J. Robot. Research*, vol. 30, no. 7, pp. 846-894, Jun. 2011.

[11] S. Cho and S. Jo, "Incremental online learning of robot behaviors from selected multiple kinesthetic teaching trials," *IEEE Trans. Syst. Man Cybern. B, Cybern.*, vol. 43, no. 3, pp. 730-740, Sep. 2013.

[12] B.-S. Yoo and J.-H. Kim, "Fuzzy integral-based gaze control of a robotic head for human robot interaction," *IEEE Trans. Cybern.,* to be published.

[13] M. A. Fischler and R. C. Bolles, "Random sample consensus: A paradigm for modeling fitting with applications to image analysis and automated cartography," *Commun. ACM,* vol. 24, no. 6, pp. 381-395, Jun. 1981.

[14] W.-R. Ko and J.-H. Kim, "Behavior selection method of humanoid robots to perform complex tasks," in *Proc. Int. Conf. Robot Intelligence Technology and Applications*, Beijing, China, 2014, pp. 127-133.

[15] M. Sugeno, "Fuzzy measures and fuzzy integrals: A survey," in *Proc. Fuzzy Automata and Decision Processes*, vol. 78, no. 33, M.M. Gupta, G.N. Saridis and B.R. Gaines, eds. Amsterdam, The Netherlands: North-Holland, 1977, pp. 89-102.

[16] S.-J. Lee *et al.,* "Arm trajectory generation based on RRT* for humanoid robot," in *Proc. Int. Conf. Robot Intelligence Technology and Applications,* Beijing, China, 2014, pp. 373-383.

[17] Y. Ye and J. Tsotsos, "A complexity-level analysis of the sensor planning task for object search," *Comput. Intell.,* vol. 17, no. 4, pp. 605-620, Nov. 2001.

[18] B.-J. Lee *et al.,* "Modifiable walking pattern of a humanoid robot by using allowable ZMP variation" *IEEE Trans. Robot.*, vol. 24, no. 4, pp. 917-925, Jul. 2008.